

Technical University of Denmark



On-line non-contact gas analysis

Fateev, Alexander; Clausen, Sønnik

Publication date:
2008

Document Version
Publisher's PDF, also known as Version of record

[Link back to DTU Orbit](#)

Citation (APA):
Fateev, A., & Clausen, S. (2008). On-line non-contact gas analysis. Roskilde: Danmarks Tekniske Universitet, Risø Nationallaboratoriet for Bæredygtig Energi. (Denmark. Forskningscenter Risoe. Risoe-R; No. 1636(EN)).

DTU Library

Technical Information Center of Denmark

General rights

Copyright and moral rights for the publications made accessible in the public portal are retained by the authors and/or other copyright owners and it is a condition of accessing publications that users recognise and abide by the legal requirements associated with these rights.

- Users may download and print one copy of any publication from the public portal for the purpose of private study or research.
- You may not further distribute the material or use it for any profit-making activity or commercial gain
- You may freely distribute the URL identifying the publication in the public portal

If you believe that this document breaches copyright please contact us providing details, and we will remove access to the work immediately and investigate your claim.

On-line non-contact gas analysis

Alexander Fateev, Sønnik Clausen

Risø-R-1636(EN)



Author: Alexander Fateev, Sønnik Clausen
Title: On-line non-contact gas analysis

Risø-R-1636(EN)
March 2008

Abstract (max. 2000 char.):

ISSN 0106-2840
ISBN 978-87-550-3659-8

Non-intrusive and fast measurements of the gas temperature, NO and other gas concentrations at elevated temperatures in boilers, engines and flames are of the great interest. The optical properties of the gases must be known in a spectral range and temperature level of interest. High-resolution IR- and UV-absorption spectra of the NO have been measured with a hot gas cell operated from the ambient up to 1400 – 1500 °C. Similarly, high-resolution infrared absorption spectra of the H₂O have been measured. Measurements are compared with simulated spectra using the HITRAN-2006 and HITEMP-1996 databases, and good agreement has been found for NO (e.g. deviations of 1-5% for NO at 1200 °C). Practical high-resolution measurements at the AVV2 boiler are analysed, and detection limits for the NO are discussed. The developed tools and results will be used in the future projects, e.g. fast measurements of the gas composition in the near-burner field with co-firing of biomass and coal, and NO measurements in a large diesel engine.

Contract no.:
Energinet.dk nr. 2006 1 6382

Group's own reg. no.:
PSP 1750175-01

Sponsorship:

Cover :
The UV optical head mounted on the end of the 9-m long water-cooled probe. Light emerging from a UV-lamp passes a distance around 20 cm before it is collected by a fused-silica lens onto a quartz fibre coupled to a UV spectrometer.

Abstract (in Danish)

Berøringsløse, hurtige optiske målinger af NO og andre gaskoncentrationer ved høj temperatur i fyrrum, flammer og motorer har generelt stor interesse. En optisk måling af NO forudsætter at de optiske egenskaber er kendt i et relevant spektral- og temperaturområde, f.eks. ud fra målinger eller databaser. I dette projekt er NO's infrarøde (IR) og UV absorptionspektra udmålt i Risø DTU's højtemperaturgascelle fra stuetemperatur op til 1400 – 1500 °C. Desuden er der foretaget målinger af H₂O IR-spektra med hensyn til interferens. Målinger på gascelle er sammenlignet med simulerede spektre ud fra HITRAN-2006 og HITEMP-1996 som viser god overensstemmelse i udvalgte spektralområder, f.eks. er afvigelser blot 1-5 % for NO ved 1200 °C. En forsøgsmåling på AVV2 kedel er foretaget og analyseret, og detektionsgrænser for NO er diskuteret. Resultater og udviklede værktøjer i projektet vil blive anvendt i fremtidige projekter, f.eks. gasmåling i nærbrænderfelt ved samfiring af halm og kul og hurtige optiske målinger af NO i skibsmotor.

Pages: 22
Tables: 3
References: 11

Information Service Department
Risø National Laboratory
Technical University of Denmark
P.O.Box 49
DK-4000 Roskilde
Denmark
Telephone +45 46774004
bibl@risoe.dk
Fax +45 46774013
www.risoe.dtu.dk

Contents

Preface 4

1 Introduction 5

2 Theory 6

2.1 Spectra calculation using IR HITRAN/HITEMP databases and UV f_{ν} data 6

2.2 Doppler and collision broadenings 8

3 Experimental set up 10

4 Experimental results and discussion 13

4.1 IR high-resolution NO absorption measurements in HGC 13

4.2 IR high-resolution H₂O absorption measurements in HGC 14

4.3 IR high-resolution measurements at AVV2 16

4.4 UV high-resolution NO absorption measurements in HGC 17

4.5 Test of 9-m long probe with UV optical head at AVV2 18

5 Conclusions 21

6 References 22

Preface

The report describes the work carried out in the PSO Project 6382. Optical properties of NO in the UV and IR spectral regions have been studied from 23 °C to 1400/1500 °C. Methods, results and experience from the project will be applied in future projects for practical *in situ* optical measurements of NO, e.g. in a large-scale boiler flame with straw co-firing (PSO Project 7333) and in a large diesel ship engine (FP7 Project “HERCULES-B”).

Further details can be found in the near future in publications related to this project, i.e. the work related to non-contact measurement of NO in combustion systems.

1 Introduction

Non-contact gas analysis of hot gas flows by optical methods is a powerful tool for measurement of the gas temperature and the gas composition inside boilers, particle loaded hot gas flows, flames and engines. In previous projects, Risø DTU has successfully demonstrated *in situ* simultaneous optical measurements of the gas temperature and species concentrations (e.g. CO, CO₂, H₂O and C_xH_y) with the use of the FTIR emission spectroscopy in boilers and flames. Gas concentrations can be directly measured in large-scale combustion systems with a water-cooled 3 – 9 m long fibre optic probe inserted or by cross-stack measurements over 2 – 20 m. Optical measurements of the NO in the infrared (IR) spectral region are difficult as the NO concentration is usually low, the spectrum of the NO is overlapped with H₂O vapours and an absorption signal (at elevated temperatures) is decreased. A spectral resolution of 2 cm⁻¹ is normally used in practical fast Fourier Transform Infrared (FTIR) measurements inside the boilers; however, a higher resolution, e.g. 0.125 cm⁻¹, may be also used in order to improve the distinction between the NO features and the H₂O lines and find the best regions for NO detection where there is minimum interference with H₂O lines.

In this work, the NO laboratory high-resolution absorption spectra are obtained and compared with simulated spectra with the use of the HITRAN-2006 spectroscopic database at temperatures up to 1400 °C. Measurements were performed on the third generation of the hot ceramic flow gas cell (HGC) that was established in the PSO F&U Project 5348, see Table 1. The performance of the HGC has been experimentally validated by comparison of the CO₂ absorption spectra measured at 1000 °C in the HGC with the same spectra measured at the same temperature on the old gas cell with hot sapphire windows.

Table 1. An overview of the hot gas cells parameters at Risø DTU.

| | SS gas cell | Ceramic gas cell | Ceramic flow gas cell |
|-------------------|------------------|------------------|-----------------------|
| Temperature range | 20 – 800 °C | 20 – 1000 °C | 20 – 1600 °C |
| Pressure range | 1 bar abs | 0 – 5 bar abs | Approx. 1 bar abs |
| Optical path | 50 cm | 50 cm | 53.3 cm |
| Windows | CaF ₂ | Sapphire | No hot window |
| Spectral region | 0.2 – 8 μm | 0.3 – 6 μm | <0.2 – >200 μm |
| Aperture gas cell | Ø 45 mm | Ø 32 mm | Ø 15 mm/Ø 32 mm |
| Project | Aeroprofile, EU | Menelas, EU | PSO, energinet.dk |

The work has been extended with a detailed study of the NO UV-absorption spectra at temperatures up to 1500 °C. Optical methods for detection of NO in the UV spectral region are investigated because interference NO with the H₂O is a minor problem in the UV region and the detection limit of the NO in the UV is significantly lower than in the IR region.

A brief introduction to the theory of spectral calculations is given in the Chapter 2.

2 Theory

An experimental high-resolution rovibronic molecular spectrum shows (at sufficient resolution) a set of rotational lines. Adequate modelling of the high-resolution molecular spectra requires knowledge about intensities for most of all rotational lines. Intensity of each line can essentially be characterized by its integral line strength, $S_{J'J''}^{v'v''}$, that can be obtained from either sophisticated experiments or from *ab initio* calculations. The line strength can be also expressed in terms of oscillator strength, $f_{v'v''}$. In Section 2.1, a general approach for calculation of a high-resolution IR/UV-absorption spectrum based on HITRAN/HITEMP databases and available $f_{v'v''}$ data is discussed. In Section 2.2, calculation of a line shape function for a single rotational line is described.

2.1 Spectra calculations using IR HITRAN/HITEMP databases and UV $f_{v'v''}$ data

The integral line intensity for the two states of the vibronic/rovibronic molecular system is defined as

$$S_{J'J''}^{v'v''}(T) \propto N_{v''J''}(T) B_{v''J''}^{v'J'} \nu_{v''J''}^{v'J'}, \quad (1)$$

where $B_{v''J''}^{v'J'}$ is the Einstein absorption coefficient, $N_{v''J''}(T)$ is the population of the ground $v''J''$ level at the temperature T , and $\nu_{v''J''}^{v'J'}$ is the frequency of an optical transition. Assuming a local thermodynamic equilibrium, the $S_{J'J''}^{v'v''}$ can finally be expressed as the product of a function of the temperature and the transition moment. In many applications and in particular in atomic/molecular absorption spectroscopy, the transition moment is replaced by dimensionless quantity - oscillator strength, $f_{v'v''}$. The transition moment, or the oscillator strength, reflects a fundamental molecular property to absorb light and does not depend on the temperature. For many molecules having strong interest in atmospheric/planetary research, information about $S_{J'J''}^{v'v''}$ at a reference temperature 23 °C is collected in the HITRAN database [1]. Calculations of other temperatures can be performed by temperature correction of the $S_{J'J''}^{v'v''}$ values. Most of the HITRAN $S_{J'J''}^{v'v''}$ data relate to IR spectroscopy. The HITRAN database is periodically updated taking account of the progress in the experiments and calculations. In the present work, HITRAN-2004 with 2006 year update for several molecules has been used. The HITRAN database is successfully used for modelling of the absorption spectra of many abundant atmospheric molecules such as H₂O, CO₂, NO and CO at low and moderate temperatures (< 200 °C). Deviations between calculations and observed absorption spectra become significant at high temperatures (> 500 °C). The 1996 edition of HITRAN contains a high-temperature database (reference temperature 800 °C) for CO, CO₂ and H₂O called HITEMP. In the present work the HITEMP-1996 database was used.

An NO UV-absorption spectrum can be modelled with the use of the $f_{v'v''}$ values. A recent compilation on the $f_{v'v''}$ values for several NO UV-absorption bands and its comparison with previously published data was presented in Ref. [2]. In general, the ratio of $f_{v'v''}$, $S_{J'J''}^{v'v''}$,

absorption coefficient, $k_{J',J''}^{v',v''}(\nu, T)$ to absorption cross section, $\sigma_{J',J''}^{v',v''}(\nu, T)$, can be expressed by the following equations:

$$\int_{line} k_{J',J''}^{v',v''}(\nu, T) d\nu \propto f_{v',v''} \frac{S_{J',J''}}{2J''+1} N_{v'',J''}(T) \propto S_{J',J''}^{v',v''}(\nu, T) N, \quad (2)$$

$$\sigma_{J',J''}^{v',v''}(\nu, T) = \frac{k_{J',J''}^{v',v''}(\nu, T)}{N}, \quad (3)$$

where $S_{J',J''}$ is the Hönl-London factor that could be calculated for various transitions, and N is the molecular number density.

The spectral distribution of the absorption cross section is given by:

$$\sigma_{J',J''}^{v',v''}(\nu, T) \propto V(\nu - \nu_0, T) S_{J',J''}^{v',v''}(\nu, T), \quad (4)$$

or

$$\sigma_{J',J''}^{v',v''}(\nu, T) \propto V(\nu - \nu_0, T) f_{v',v''} \frac{S_{J',J''}}{2J''+1} \frac{N_{v'',J''}(T)}{N}, \quad (5)$$

where $V(\nu - \nu_0, T)$ is a normalized line-shape function that is determined by various broadening effects (e.g. Doppler or collision broadenings), $\int V(\nu - \nu_0, T) d\nu = 1$. In the high-temperature (and pressures around atmospheric) applications, $V(\nu - \nu_0, T)$ can be assumed to be as the Voigt function (see below).

In the majority of the practical applications an instrument line-shape function (ILS), $f(\nu - \nu_0)$, of, for example, FTIR- or UV-spectrometers affects the observed absorption cross sections. An experimentally measured absorption spectrum relates to an apparent absorption cross section, $\sigma_{J',J''}^{v',v''}(\nu, T)^{app}$, and to the “true” absorption cross section, $\sigma_{J',J''}^{v',v''}(\nu, T)$, by the following relations:

$$\ln \left[\frac{I_0(\nu)}{I(\nu)} \right] = \sigma_{J',J''}^{v',v''}(\nu, T)^{app} l N, \quad (6)$$

and

$$\sigma_{J',J''}^{v',v''}(\nu, T)^{app} = \int f(\nu - \nu_0) \sigma_{J',J''}^{v',v''}(\nu, T) d\nu, \quad (7)$$

$$\int f(\nu - \nu_0) d\nu = 1$$

where $I_0(\nu)$ and $I(\nu)$ are the reference and the detected light intensities, respectively, and l is the absorption optical path length. In case of UV-absorption calculations, ν (cm^{-1}) in Eqs. (6) and (7) should be replaced by λ (nm). The quantity in the right-hand side in Eq. (6) is called the apparent optical depth, OD^{app} .

A calculation of the absorption spectrum at certain values of T , N and l is done through the following steps: (1) calculation of $V(\nu - \nu_0, T)$ (see below); (2) calculation of $\sigma_{J',J''}^{v',v''}(\nu, T)$ based on $S_{J',J''}^{v',v''}$ (Eq. (4)) or $f_{v',v''}$ (Eq. (5)) known values from the HITRAN/HITEMP database or from Ref. [2]; (3) calculation of the “true” absorption spectrum, $k_{J',J''}^{v',v''}(\nu, T) l$, Eqs. (2) and (3), and (4) either calculation of the “apparent” cross sections, Eq. (7), or the “apparent” absorption spectrum, Eq. (6) based on known ILS. In IR- and UV-absorption calculations, sinc^2 (FWHM=0.125 cm^{-1}) and triangular-like (FWHM=0.046 nm), respectively, ILS functions were used.

2.2 Doppler and collision broadenings

Thermal particle motion causes well-known Doppler line broadening, and mutual particle interaction leads to collision (Lorentz) broadening. These are two major importance mechanisms of a single rotational line broadening in the hot gases. The line profile of an absorption line is defined by a normalized line-shape function $V(\nu - \nu_0, T)$ mentioned in the previous section. Assuming that the mechanisms of Doppler and impact broadening are statistically independent the line-shape of a single line can be described by symmetric and shifted normalized Voigt profile and appears as [3, 4]:

$$V(\nu - \nu_0, T) = \frac{2\sqrt{\ln 2/\pi}}{\Delta\nu_D} u(y - s, a), \quad (8)$$

where $\Delta\nu_D$ is the Doppler width,

$$\Delta\nu_D = 7.1623 \cdot 10^{-7} \nu_0 \sqrt{\frac{T}{M(\text{amu})}}, \quad (9)$$

where ν_0 is the unshifted centre frequency, $u(y-s, a)$ is the Voigt function, y is the normalized collision frequency $2\sqrt{\ln 2} \frac{(\nu - \nu_0)}{\Delta \nu_D}$, s is the normalized collision shift $2\sqrt{\ln 2} \frac{\Delta \nu_s}{\Delta \nu_D}$, and a is the Voigt parameter,

$$a = \sqrt{\ln 2} \frac{\Delta \nu_c}{\Delta \nu_D} \quad (10)$$

through which the contributions of collision and Doppler broadening are compared.

In a multicomponent system in the binary-collision regime the total collision width is expressed as

$$\Delta \nu_c = p \sum_i X_i 2\gamma_i, \quad (11)$$

where p is the total pressure, X_i is the mole fraction of the i^{th} component and $2\gamma_i$ is the collision shift per unit pressure induced by species i . Defining $2\delta_i$ as the collision shift per unit pressure induced by species i , a similar expression can be used for the total collision shift [4]:

$$\Delta \nu_s = p \sum_i X_i 2\delta_i \quad (12)$$

Usually values of the collision width and shift are known for a reference temperature, T_0 . The temperature dependence for both $2\gamma_i$ and $2\delta_i$ is expressed by

$$2\gamma_i = 2\gamma_i^{T_0} \left[\frac{T_0}{T} \right]^{m_i} \quad (13)$$

and

$$2\delta_i = 2\delta_i^{T_0} \left[\frac{T_0}{T} \right]^{n_i} \quad (14)$$

with temperature exponents m_i and n_i for species i [5].

If the temperature is increased (at constant total pressure), the Doppler width is increased too as $\Delta\nu_D \propto T^{0.5}$, Eq. (9); however, the Lorentz width becomes less as $\Delta\nu_c \propto T^{-n}$ ($0.5 < n < 1$), Eq. (13). As a result, the Voigt a parameter becomes less, Eq. (10) or, in other words, the lines become narrower.

Pressure broadening parameters γ_i for many IR-active gases (as the self- and air-broadening halfwidths) together with temperature exponents m_i and n_i have been tabulated in HITRAN/HITEMP databases. For NO UV-absorption calculations, collision broadening parameters have been summarized in Ref. [6]. Prior calculations of the available line-by-line rotational line-broadening parameters from HITRAN/HITEMP databases were averaged and these averaged values have been used in calculations of a line profile. In UV calculations, line-broadening parameters were assumed to be the same for all rotational lines in two NO vibronic absorption bands. The line profile $V(\nu - \nu_0, T)$ was numerically calculated for all molecules under investigation for all temperature settings used in the experiments. The calculations were performed fulfil the condition: $\int V(\nu - \nu_0, T) d\nu = 1$.

3 Experimental set-up

Measurements have been performed on our newly developed atmospheric-pressure high-temperature flow gas cell (HGC), Fig. 1 [7]. The gas cell was designed as a flow gas cell with a so-called laminar window, nozzle seal cell principle, where care was taken to obtain a similar uniform gas temperature profile and well defined path length as for the other two gas cells with hot windows in our laboratory.

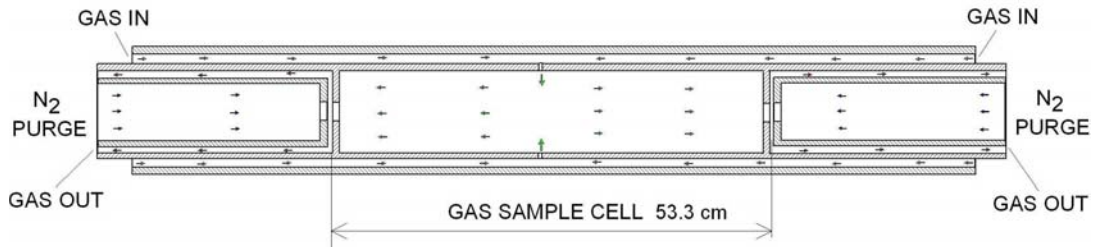


Figure 1. High-temperature flow gas cell (HGC) used in the experiments. Arrows show directions of the gas flows. See text for more explanations.

The HGC consists of three different parts: a high-temperature sample cell with a length of 0.533 m and two “buffer” cold gas parts on the left- and the right-hand sides of the hot sample cell. The buffer parts are filled by a UV/IR-transparent (purge) gas (e.g. N_2), whereas the central sample cell can be filled by the gas under investigation (e.g. N_2+H_2O/NO). The aperture of the sample cell is kept small (i.e. a diameter of 0.015 m) in order to reduce heat transfer by radiation from the sample cell and to reduce the risk of collapse of well-defined flows in the laminar windows. The laminar windows also function as a radiation shield. Similarly, apertures placed at the end parts between the laminar windows and the cold windows reduce the heat losses by radiation and convection by breaking down the vortices created by the thermal gradient in the buffer sections. High-quality pure ceramics were used in order to minimize hetero-phase reactions and to avoid contact of the sample gas with any hot metal parts. A uniform temperature profile is obtained by heating the gas cell with a dedicated three-zone furnace in order to compensate for the heat loss at the ends of the gas cell. The sample gas is

preheated. Flows of the gases in the sample cell and in the buffer parts are kept at about the same flow rates. The outer windows placed on the ends of the buffer parts are replaceable. In all experiments, KBr-windows have been used. The gas flow through the HGC maintains a highly uniform and stable temperature in the range 23 °C to 1500 °C.

The HGC performance has been carefully tested by flow visualization calculations and by IR emission/absorption measurements for various temperatures in the sample cell and gas flows in the sample cell and in the buffer parts. Further details of the experimental set-up will be presented and discussed in another paper [8].

High-resolution IR-absorption measurements were performed with an advanced FTIR-spectrometer (Nicolet model 5700) equipped with various IR-detectors: DTGS, InSb and MCT. Because the MCT detector has shown highly nonlinear behaviour at all signal levels, only two former MCT detectors were used. The nominal resolution of FTIR, $\Delta\nu$, was 0.125 cm^{-1} and was sufficient in order to observe in a fine-structure absorption (single rotational lines) of NO, CO and H₂O molecules.

A highly stable calibrated blackbody operated at 800 °C was utilized as an IR light source for absorption and calibration measurements. After passing through the HGC, the IR light beam was restricted by a variable aperture to minimize possible surface effects in the HGC with following pass through the Jacquinot-stop system mounted on the outer part of the Nicolet spectrometer operated in the external light source mode.

High-resolution UV-absorption measurements were performed with a 0.5 m UV/VIS-spectrometer (Acton Research) equipped with a UV-optimized holographic grating (1200 grooves·mm⁻¹) and a UV-enhanced PIXIS CCD-camera with 1340x100 pixels (Princeton Instruments). The dispersion of the grating was sufficient to observe a range of 28 nm on the CCD, allowing simultaneous recording (without movement of the grating) of three UV γ -absorption bands of NO ($A^2\Sigma^+ \leftarrow X^2\Pi$): $A, v'=1 \leftarrow X, v''=0$, $A, v'=0 \leftarrow X, v''=0$ and $A, v'=0 \leftarrow X, v''=1$. A spectral resolution of $\Delta\lambda=0.048$ nm for all UV-absorption measurements with the 0.5 m UV/VIS spectrometer was achieved with an entrance slit width of 20 μm .

A highly stable deuterium lamp (Oriel Instruments) with a UV-condenser was utilized as a parallel-beam light source in the range 190-400 nm. After passing through the HGC, the UV light beam was focused by means of a short-focal-length CaF₂-lens into the head of a 0.5 m long fused-silica optical fibre coupled to the entrance slit of the UV/VIS spectrometer. The uncorrected spectrum of the deuterium lamp/fibre combination over 190-400 nm presents continuum-like behaviour with a broad maximum at 240-250 nm decreasing to zero at around 180 nm due to the transmission limitations of the CaF₂ lens, the optical fibre, and the diminishing sensitivity of the spectrometer + CCD system.

In the experiments, mixtures of N₂+NO (100-6500 ppm) and N₂+H₂O (1-40 %) at a flow rate about 2 l_n·min⁻¹ have been used. Calibrated mass-flow controllers were applied to control the gas flows. Different NO concentrations were obtained by flow mixing of N₂ and N₂+NO (1 %) gases at different N₂:N₂+NO (1 %) ratios. UV-absorption measurements were performed at four different temperatures: 23 °C, 500 °C, 1000 °C and 1500 °C. In H₂O IR-absorption measurements an accurate HAMILTON syringe pump system with a water evaporator was used.

Gas temperature and temperature uniformity along the axis of the high-temperature central part of the HGC were verified by thermocouple measurements at three different points inside the HGC, and by IR-emission/absorption measurements of the N₂+CO₂ (1 %) gas mixture [9] in a separate set of measurements before the NO absorption experiments. The temperature uniformity over 0.45 m was found to be better than ± 1 °C, or on average ± 0.5 °C.

Table 2. Summary of high-resolution NO IR-absorption measurements. See text for the details.

| | 23 °C | 500 °C | 800 °C | 1000 °C | 1200 °C | 1400 °C |
|---|-----------------------------|--------|-----------------------|-----------------------|---------|---------|
| $\Delta\nu=0.125\text{ cm}^{-1}$ | N ₂ + NO(.. ppm) | | | | | |
| NO vol ppm | 878 | 978 | 978,3170,6458 | 978,3170 | 3170 | 3170 |
| $\Delta[\sigma(\nu)\Delta\nu]$, % exp1-exp2 | - | 0.3 | 14.4* | 3.9* | 1.1 | 1.9 |
| $\Delta[\sigma(\nu)\Delta\nu]$, % exp-clc ^{HITRAN} | 4.1 | 1 | 2.1 ^{3170**} | 4.8 ^{3170**} | 4.8 | 4.7 |
| # points line ⁻¹ | 8-12 | 3-4 | 3-5 | 2-3 | 2-3 | 1-3 |
| $\Delta\nu^{\text{Voigt}}$, cm ⁻¹ | 0.099 | 0.050 | 0.041 | 0.037 | 0.034 | 0.032 |

*) spectra with two different NO concentrations used

**) NO concentration (ppm) used for calculations

Table 3. Summary of high-resolution H₂O IR-absorption measurements. See text for the details.

| | 23 °C | 500 °C | 800 °C | 1000 °C | 1200 °C | 1400 °C |
|---|---|--------|-------------------|---------|--------------------|---------|
| $\Delta\nu=0.125\text{ cm}^{-1}$ | N ₂ + H ₂ O(.. %) | | | | | |
| H ₂ O vol % | - | 8 | 10,35,40 | 35 | 35,40 | 35 |
| $\Delta[\sigma(\nu)\Delta\nu]$, % exp1-exp2 | - | - | 2.6 | - | 5 | - |
| $\Delta[\sigma(\nu)\Delta\nu]$, % exp-clc ^{HITEMP} | - | 2 | 3.2 ^{4*} | 7.5 | 11.6 ^{2*} | 9 |
| # points line ⁻¹ | - | 10-12 | 6-8 | 6-8 | 6-8 | 4-6 |
| $\Delta\nu^{\text{Voigt}}$, cm ⁻¹ | 0.2506 | 0.1834 | 0.1499 | 0.1362 | 0.1262 | 0.0914 |

*) number of experimental spectra used in calculations

4 Experimental results and discussions

Various experiments have been performed. High-resolution, high-temperature IR NO and H₂O absorption measurements in HGC are presented and discussed in Sections 4.1 and 4.2. A summary of the NO/H₂O measurements is presented in Tables 2 and 3. In Section 4.3 results of the first high-resolution, large-scale IR-emission measurements are presented, and the NO detection limit in practical applications is evaluated and discussed. The following two sections describe the extension of the *in situ* optically based technique into the UV spectral range. In Section 4.4 high-resolution NO UV-absorption measurements at high temperatures are presented. In Section 4.5, *in situ* fast UV-absorption measurements 8 m inside of high-temperature region of a large scale industrial boiler with unique water-cooled probe are to our knowledge reported for the first time. The NO detection limit in the fast UV-absorption measurements are evaluated and discussed.

4.1 IR high-resolution NO absorption measurements in HGC

The NO high-resolution IR-absorption measurements were performed at various NO concentrations and temperature settings. An overview of the measurements is presented in Table 2. A liquid N₂-cooled InSb detector was used in most of the measurements. It was verified that the Lambert-Beer law remains valid at NO concentrations up to 4000 ppm (800 °C). An example of NO IR-absorption spectrum at 1200 °C and NO = 3170 ppm measured in HGC is shown in Fig. 2. The spectrum was calculated to the apparent absorption cross-section scale (cm² molecules⁻¹) as was described in Section 2.2.

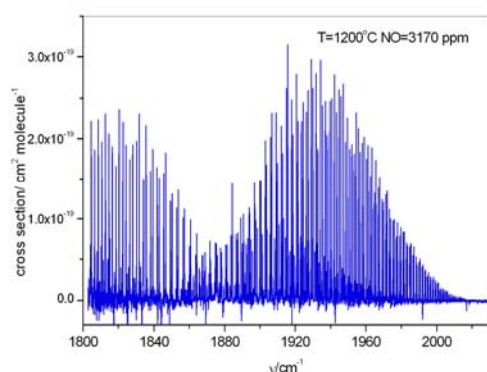


Figure 2. An example of NO high-resolution IR-absorption spectrum in HGC. NO= 3170 ppm, T= 1200 °C.

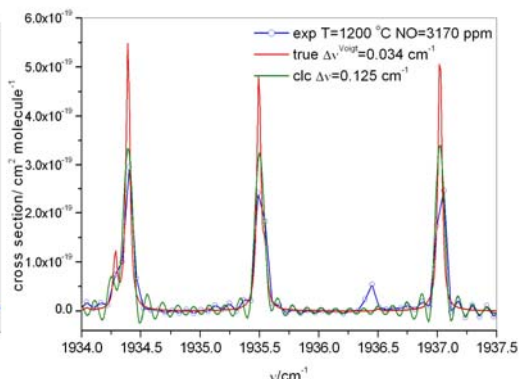


Figure 3. A part of the spectrum in Fig. 2 (opened circles, blue line), true absorption (red) and calculated (olive) spectra. See text for the details.

In Fig. 3, a part of the high-resolution spectrum in Fig. 2 is shown in more details. The “true” absorption spectrum is only defined by a Voigt function with $\Delta\nu^{Voigt} = 0.034 \text{ cm}^{-1}$ (FWHM) shown by the red line. The “apparent” absorption spectrum (red line) was calculated based on the HITRAN-2006 database, $T = 1200 \text{ °C}$ and the boxcar apodization function as described in Sections 2.1 and 2.2.

As was mathematically demonstrated in [4], the instrument resolution influences the apparent cross-sections measured. In general, the instrumental spectral resolution (FWHM) should be less than one fifth of the absorption linewidth (FWHM) in order to obtain the true value of the cross-section [4]. Because our instrumental resolution, $\Delta\nu=0.125\text{ cm}^{-1}$, is higher than the absorption linewidth, $\Delta\nu^{Voigt}$, calculated (and observed) spectra show less values in the maxima of the absorption lines. However, the integral values of the “apparent” cross-sections, $\int_{line} \sigma_{J'J''}^{\nu\nu''}(\nu, T)^{app} d\nu$, used in our work do not depend on the instrumental resolution and they are equal to the integral value of the “true” absorption cross-section only determined by Doppler and Lorentz broadenings. Due to the sampling algorithm of the FTIR spectrometer software, each rotational line of NO is described by 2-3 points in the spectra ($T = 1200\text{ }^{\circ}\text{C}$), see Table 2 and Fig. 3, whereas in the calculations a line can be described by more points. That explains the difference of 4.8 % in the integral cross-sections between the calculations and experiment, see Table 2. An uncertainty in the experimental spectra recorded one –by one is less: 1.1%. On the other hand, it should be noted that the HITRAN-2006 database used in our calculations was developed for atmospheric research purposes at low and moderate temperatures ($< 200\text{ }^{\circ}\text{C}$). In general, the discrepancy between calculations and experimental data lies in the range 1-5 % for $23\text{ }^{\circ}\text{C} < T < 1400\text{ }^{\circ}\text{C}$ and in our opinion that is excellent.

4.2 IR high-resolution H₂O absorption measurements in HGC

In general, water has four regions of strong absorption covering a spectral range from 200 to 6000 cm^{-1} . In high-temperature practical applications (e.g. inside large scale boilers), the NO absorption band at $\nu_0 = 1870\text{ cm}^{-1}$ is strongly overlapped with the second H₂O band (1000-2500 cm^{-1}). Due to differences in absorption cross-sections, H₂O (a few per cent) and NO (a few hundreds ppm) concentrations, NO absorption shows very weak features on the “strong” H₂O absorption background. Therefore the quality of reference H₂O absorption spectra is a key issue in the following determination of the NO concentration. Water high-temperature absorption data are lacking in literature due to at least two reasons: (1) not all laboratories may have reliable measurements of water absorption at high temperatures and (2) adequate theoretical modelling of the water absorption at high temperatures needs involving a huge set of basic functions and it is a burden to consider various types of couplings, thus making calculations very complex and time consuming. Because the high water content in real high-temperature applications (5-10 %), water absorption bands always show saturation. However, there are regions, where for several H₂O rotational lines the absorption is governed by Lambert-Beer law and these lines may therefore be used for evaluation of the water content and the following NO concentration. A summary of our high-resolution H₂O IR-absorption measurements is presented in the Table 3.

Water absorption can be modelled by the approach described in Sections 2.1-2.2 that uses the HITRAN-2006 database or its extension to the high temperature range (800 $^{\circ}\text{C}$) HITEMP-1996 database. In Figs. 4 and 5 experimental spectra at two different temperatures: $T = 800\text{ }^{\circ}\text{C}$ and 1200 $^{\circ}\text{C}$, respectively, H₂O = 35% opened circles (blue line) together with their fitting based on HITRAN-2006 (olive line) and HITEMP-1996 (red line) in the range of NO absorption interest are shown.

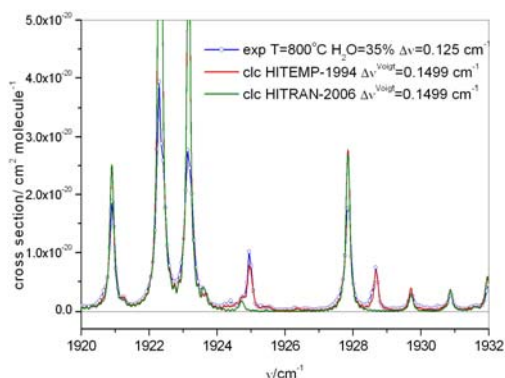


Figure 4. A part of the H_2O IR-absorption spectrum (opened circles, blue line), HITRAN (olive) and HITEMP (red) calculated spectra. $T = 800$ °C, $H_2O = 35\%$.

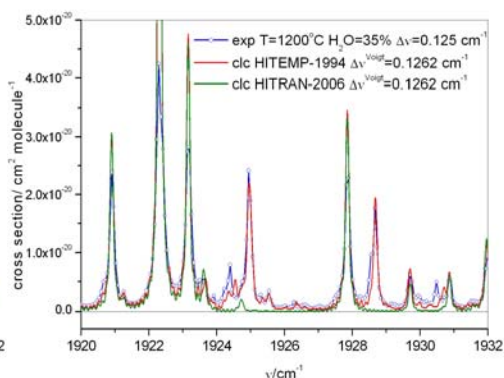


Figure 5. A part of the H_2O IR-absorption spectrum (opened circles, blue line), HITRAN (olive) and HITEMP (red) calculated spectra. $T = 1200$ °C, $H_2O = 35\%$.

The experimental spectrum was calculated to the absorption cross-section scale ($\text{cm}^2 \text{molecule}^{-1}$). As can be seen, the HITEMP-1996 database used in the calculations allows us to make a significantly better fit to the experimental spectra compared with the use of the HITRAN-2006. However, a deviation between the experiment and the calculations becomes more pronounced if the temperature is raised, see Fig 5. In Table 3, discrepancies in the integrated absorption cross-sections from the experimental absorption spectra and HITEMP-1996 based calculations in the range 1924.04 - 1931.51 cm^{-1} at various temperatures are summarized. The discrepancy is in the range 2-12% that is very acceptable taking into account that HITEMP-1996 was developed for temperatures around 800 °C.

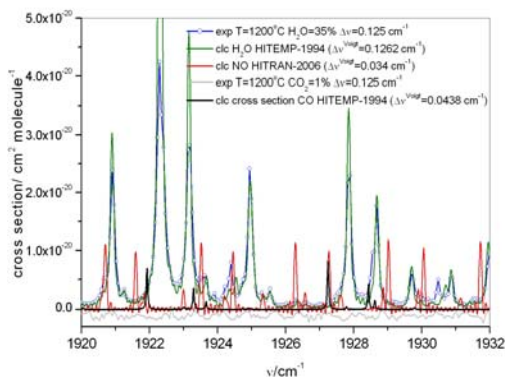


Figure 6. Experimental H_2O (opened circles, blue line) and CO_2 (light grey) cross sections, calculated H_2O (HITEMP, blue line), NO (HITRAN, red) and true CO (HITEMP, black) cross sections at $T = 1200$ °C.

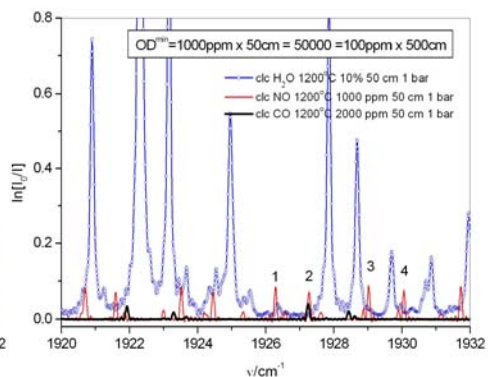


Figure 7. Calculated IR-absorption spectra for $H_2O = 10\%$ (HITEMP, opened circle, blue), $NO = 1000$ ppm (HITRAN, red) and $CO = 2000$ ppm (HITEMP, black), $T = 1200$ °C.

NO absorption lines placed in the same spectral range are shown in Fig. 6 (red line). In those narrow spectral ranges where there is an overlap between NO rotational lines and H₂O “background”, the agreement between the experimental data and calculations (HITEMP-1996) is very good, see Fig. 6. Therefore, in a real complex spectrum at the positions of NO lines the HITEMP-1996 database can be used in order to subtract water features. Other combustion gases like CO (black line) and CO₂ (light grey) have a minor influence on NO features in the mentioned spectral range, see Fig. 6.

A simulated 10 % water absorption spectrum over a 50 cm optical path length at 1200 °C is shown in Fig. 7 (blue line, opened circles). The calculated NO absorption spectrum (red line) corresponding to 1000 ppm is shown by the red line in Fig. 7. The NO absorption features marked 1, 3 and 4 can be used for evaluation of NO concentration whereas absorption feature 2 overlapped with the CO rotational line. In general, it is possible to find other spectral regions (e.g. 1939-1961 cm⁻¹) where NO absorption features will dominate (at certain OD^{app} values) over H₂O “background”. The apparent optical depth can be used for evaluation of the detection limit, OD^{min} , in the IR-absorption measurements. Thus, in the case shown in Fig. 7 the OD^{min} is equal to 50000, i.e. at least 5 m optical pathlength for 100 ppm NO detection. If the temperature is lower, for example 1000 °C, then OD^{min} is less (40000), and for the detection 100 ppm of NO path length at least 4 m is required. Such long path lengths can be achieved in large-scale boilers.

4.3 IR high-resolution emission measurements at AVV2

In order to prove applicability of the high-resolution ($\Delta\nu = 0.125 \text{ cm}^{-1}$) FTIR spectroscopy in large-scale *in situ* measurements (e.g. in industrial boilers), test IR-emission measurements at AVV2 with a 1.5-meter water-cooled probe were performed. The probe was inserted 50 cm from the boiler wall. Light from the flame was focused with a lens into the IR-fibre coupled to the external IR-port of the Nicolet FTIR spectrometer. A highly stable calibrated blackbody operated at 800 °C was utilized as an IR light source for calibration of the lens-fibre-FTIR spectrometer system. An example of the high-resolution raw emission spectrum from the coal-wood-oil flame is shown in Fig. 8. The acquisition time for the spectrum was 6 minutes.

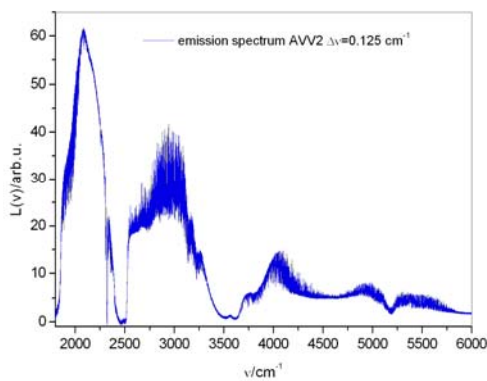


Figure 8. High-resolution emission spectrum measured at AVV2. The probe was inserted 50 cm from the boiler wall.

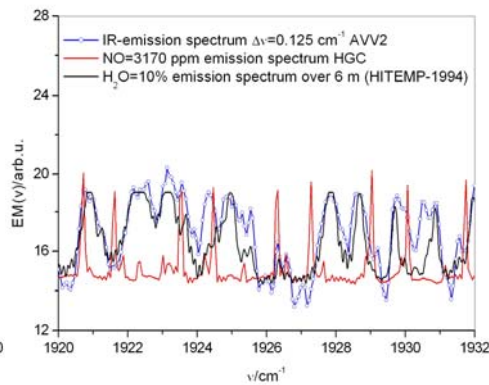


Figure 9. Corrected emission spectrum in Fig. 8 (opened circles, blue line), reference NO (3170 ppm, red) emission spectrum at $T = 1000^\circ\text{C}$ in HGC and H₂O (10 %, olive) calculated emission spectrum over 6 m (HITEMP) at $T = 1000^\circ\text{C}$.

The spectrum in Fig 8 was corrected to the “true” spectrum taking into account a (relative) transmission function of the lens-fibre-FTIR spectrometer system. A part of the corrected spectrum is shown in Fig. 9 (opened circles, blue line) together with a reference emission spectrum of NO (3170 ppm, red) measured in HGC and calculated emission H₂O (10 %, olive) over 6 m at 1000 °C based on the HITEMP-1996 database and with the same spectral resolution. All spectra are shown in arbitrary units for a more clear presentation. As can be seen from Fig. 9, the shape of the experimental spectrum measured at AVV2 follows the typical shape of the second water band, and no characteristic features caused by NO absorption between 1920 - 1932 cm⁻¹ (Fig. 7) appeared. Referring to the discussion at the end of the Section 4.2, it seems as if when measurements were performed, the NO concentration was less than 84 ppm assuming absorption pathlength 6 m (1200 °C) that is the same order as the radial size of AVV2 boiler. This observation is in agreement with data obtained from the AVV2 log-file recorded in the same time window when test experiments were done: NO^{average} = 111 ppm.

4.4 UV high-resolution NO absorption measurements in HGC

Development of a UV-absorption technique is a logical extension of our *in situ* measurement capabilities into the UV spectral range (200 - 400 nm). The UV-absorption technique has some advantages compared with the IR technique. For example, water vapour has a minor influence on the UV-absorption measurements; NO and SO₂ absorption is stronger in the UV compared with the IR range, and O₂ in-flame measurements are possible due to an expansion of the oxygen absorption to the long wavelengths with the raise of temperature. On the other hand, the IR technique is more suitable for e.g. temperature, H₂O, CO and UHC absorption measurements. In general, both techniques are complementary to each other. There is, however, one technical problem for practical implementation of the *in situ* local UV absorption measurements: the UV light source has to be safely placed in the flame. This is contrary to the IR-absorption/emission measurements where the flame itself can be used as a natural “blackbody” radiation source. However, careful design of an optical probe in practice makes it possible to overcome the problem mentioned above.

In the first UV-absorption measurements in HGC, NO has been chosen because of its high interest to combustion research. Narrow with well-recognized shape NO, UV-absorption bands are easily seen over broad absorption structures such as SO₂ or CO₂. Moreover, at sufficient spectral resolution a gas temperature can be obtained from the analysis of the fine structure of the NO bands [7]. A typical evolution of the NO UV-absorption with temperature measured in the HGC is shown in Fig. 10 for NO = 390 ppm and several temperatures from 23 °C to 1500 °C.

With a raise of temperature, NO starts to absorb at longer wavelengths and the structure of the absorption bands become broader due to Boltzmann population of the rovibronic levels with high numbers of rotational and vibrational quanta, see Figs. 10 and 11. As a result, less absorption in the maxima of the absorption bands is observed, see Fig. 11. The last effect significantly changes the NO detection limit in *in situ* UV-absorption measurements compared with the more traditional extraction UV-absorption measurements at, for example, 150 °C, see below. More discussion about high-resolution, high-temperature NO UV-absorption experiments in the HGC and modelling of the high-resolution NO spectra can be found in Ref. [7].

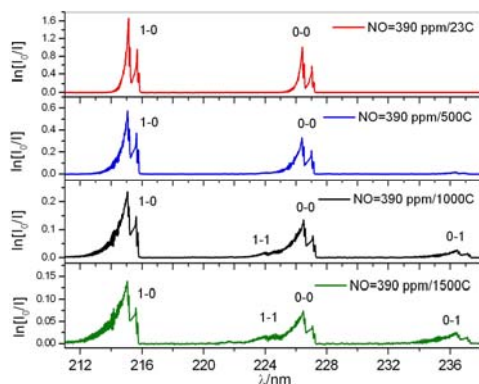


Figure 10. $\text{NO } A^2\Sigma^+ \leftarrow X^2\Pi \gamma\text{-system}$ absorption spectra in the range of 211-238 nm measured at $\text{NO} = 390 \text{ ppm}$, $l = 53.3 \text{ cm}$ and various temperatures: 23°C, 500 °C, 1000 °C and 1500 °C in HGC. Spectral resolution 0.046 nm.

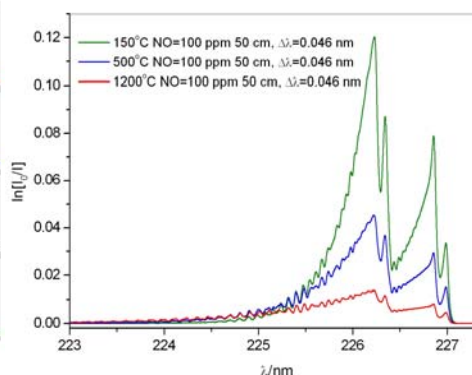


Figure 11. Calculated NO absorption spectra at 150 °C (olive line), 500 °C (blue) and 1200 °C (red). $\text{NO} = 100 \text{ ppm}$, $l = 50 \text{ cm}$. Spectral resolution 0.046 nm.

4.5 Test of a 9-m long probe with UV optical head at AVV2

The interest for local (in space) and fast (in time) *in situ* measurements of temperature and gas composition in flames on a large scale (e.g. close to a boiler wall or far inside of the boiler) is significant. These data are essential for a validation of computational modelling that is now recognized as an obligatory tool in the boiler design and optimization. As was mentioned in Section 4.3 *in situ* local UV-absorption measurements are possible if a UV-light source may be safely placed in the flame. We have developed a special 9-m long water-cooled probe with a removable UV-head for fast UV-absorption measurements far into a flame. The UV-head consists of an axial-type UV-lamp used as a light source, a pair of fused-silica lenses; one used for collimating the light from the UV-lamp and the other used for light focusing (after passing through the gas slab) into a 15-m long quartz optical fibre coupled from the other end to the Acton 0.5 m spectrometer with a CCD camera. An absorption path length in the UV-head is around 20 cm. The probe and the UV-head have successfully been tested 8 m inside the hot flame zone (1000 - 1300 °C) at AVV2. More details will be published in the coming paper [11].

A typical absorption spectrum in a coal flame measured 8 m inside the AVV2 boiler with an acquisition time of 30 ms is shown in Fig. 12 (dotted blue line). It should be noted that for the time being such a large signal noise level is caused due to (1) strong attenuation of the UV light in the 15-m long fibre used in the test measurements, (2) non-optimal choice of pair of fused-silica lenses and (3) non-optimal coupling of the optical fibre to the Acton spectrometer. In order to improve the signal-to-noise ratio, a new pair of fused-silica lenses with a shorter optical fibre and a better coupling fibre spectrometer are planned to be tested soon. An averaging over nine successive acquisitions 30 ms each ($30 \text{ ms} \times 9 = 0.27 \text{ s}$) gives a better signal-to-noise ratio, see Fig. 12 (red line).

The absorption spectra in Fig. 12 (dotted blue and red lines) correspond to a typical SO_2 absorption (second band). The shape of the SO_2 absorption spectrum depends on the temperature. Thus if the temperature increases the fine structure of the band at 280-310 nm (150 °C (black), 700 °C (grey) and 1000 °C violet lines in Fig. 12) is smeared out. The position of the local minimum between two SO_2 absorption bands (200 - 240 nm and 240 - 340 nm at 150 °C in Fig. 12) is also temperature dependent. The minimum shifts to the longer

wavelengths when the temperature is raised. Following SO_2 minimum changes with temperature based on HGC reference measurements (a part of data is shown in Fig. 12), the position of the minimum in the experimental spectrum (red line, Fig. 12) gives the value of the gas temperature 1236 °C that is typical in the region where the experiments were performed. In Fig. 12 the violet line corresponds to an absorption in the mixture $\text{NO} + \text{SO}_2$ (reduced by 1.5 for better presentation). The NO well-localized 1-0 absorption band (236 nm) is clearly seen on SO_2 “background”. It should also be noted that the 1-0 band (236 nm) is not the strongest NO -absorption feature, see Fig. 10.

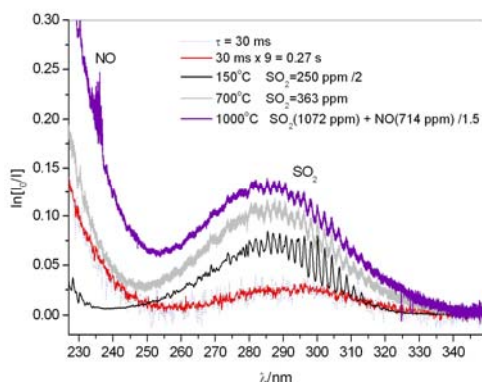


Figure 12. Fast SO_2 UV absorption measurements at AV2 (30 ms acquisition time, dotted blue line), averaging over 0.27 s (red) and $\text{SO}_2(+\text{NO})$ high-temperature absorption measurements in HGC: 700 °C (grey) and 1000 °C (violet). Sampling gas cell UV-absorption measurements: 150 °C (black).

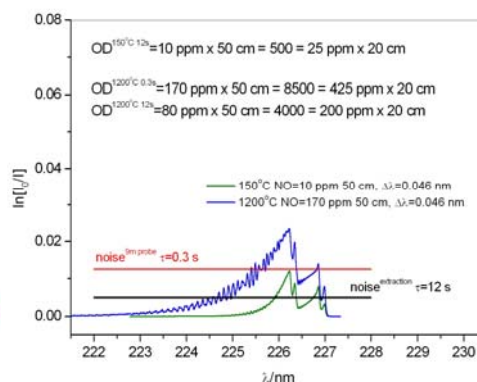


Figure 13. Calculated NO absorption spectra at 150 °C (10 ppm, olive) and 1200 °C (170 ppm, blue). $l = 50$ cm. The spectral resolution is 0.046 nm. The noise levels evaluated from Fig. 12 are shown by red (0.3 s acquisition time) and black (12 s acquisition time) lines.

Recently, the UV/IR absorption techniques have been utilized in our newly developed comprehensive system designed for isokinetic particle and gas sampling. The system includes a water-cooled probe for sampling of particles and gases with a particle filter, two 50 cm long gas cells for simultaneous UV/IR-absorption measurements, a sophisticated paramagnetic oxygen analyzer, calibrated mass-flow controllers and a pump. The data acquisition system allows us continuously to record the main sampling parameters such as sampling gas flow, gas temperature, pressure in the UV/IR gas cells and the oxygen concentration. The temperature in the sampling line (from the probe tip till the gas cells) keeps constant at 150 °C by electronically controlled heaters. The Bomem MB155 FTIR spectrometer ($\Delta\nu = 2 \text{ cm}^{-1}$) with the built-in IR light source and external DTGS detector use for IR-absorption measurements. For UV-absorption measurements a UV lamp is utilized as a light source. UV-absorption spectra record with Acton 0.5 m spectrometer ($\Delta\lambda = 0.046 \text{ nm}$) equipped with a CCD camera. A reference SO_2 absorption spectrum at 150 °C in the UV gas cell is shown in Fig. 12 (black line).

The spectra shown in Fig. 12 can be used for estimation of the NO detection limit in fast *in situ* UV-absorption measurements. The noise level can be estimated from the spectra in Fig. 12 (red and black lines). Thus, in the case of measurements in the UV gas cell (150 °C, black line), a spectrum was accumulated in $\tau = 12$ s and the estimated noise (or uncertainty) is shown in Fig. 13 by a black horizontal line. The same estimation for the averaged spectrum (red) (1236 °C,

$\tau = 30 \text{ ms} \times 9 = 0.27 \text{ s}$) gives the noise level shown by the red line in Fig. 13. The NO concentration can be evaluated if at least the top of an absorption band (above the noise level line) with the characteristic structure is clearly seen (e.g. 0-0 band at 226 nm in Fig. 13). The band structure and the band maximum both depend on the temperature, see Fig. 11. Calculated NO absorption bands at 150 °C (green) and 1200 °C (blue) give OD^{min} at relevant temperatures. Therefore, at 150 °C the $OD^{min}_{12s} = 500$, i.e. a 10 ppm NO detection limit for 12 s measurement time. At 1200 °C the $OD^{min}_{12s} = 4000$, i.e. equivalent to the 200 ppm detection limit of NO in 12 s measurement time. In contrast, fast ($< 0.3 \text{ s}$) UV-absorption measurements are more demanding in terms of signal-to-noise ratio: $OD^{min}_{12s} = 8500$, and the NO detection limit is 435 ppm at a 20 cm absorption path length. Improvement in the UV-head mentioned above will improve the NO detection limit. The SO₂ UV-absorption measurements are less demanding because the SO₂ is in general a stronger absorber compared with the NO, and SO₂ concentration are usually 2-3 times higher compared with the NO concentration (e.g. in coal combustion).

5 Conclusions

Accurate IR- and UV-absorption measurements of the NO and other gases have been obtained using the ceramic high-temperature gas facility at Risø DTU in the temperature range from ambient up to 1400 – 1500 °C.

- The HITRAN-2006 database can be used for modelling of the high-resolution, high-temperature NO IR-absorption spectra. Modelling gives agreement with an experiment within 1 – 5 %, e.g. optical measurements of the NO at 200 ppm can be performed with an uncertainty of 2 – 10 ppm using simulated spectra based on the HITRAN database at gas temperatures found in boilers.
- The HITEMP-1996 database may be used for modelling of the high-resolution, high-temperature H₂O absorption spectra in certain spectral ranges with uncertainties of 2-12 %. In the future experimental measurements of the H₂O absorption, the uncertainty can be improved, and can be used for accurate subtraction of the spectral features of H₂O in the measured spectra that will result in more accurate H₂O measurements and that will build a perfect basis for sensitive trace gas measurements at low resolution.
- At certain optical depths, NO absorption features can be distinguished from the complex absorption spectrum (e.g. NO+H₂O+CO+CO₂). NO detection limit by high-resolution IR-absorption spectroscopy is evaluated. The first large-scale, high-resolution IR-emission measurements were made and discussed.
- High-resolution UV-absorption spectroscopy can be also utilized for NO concentration measurements by *in situ* (inside of boilers) or extraction techniques. The gas temperature can be evaluated from the analysis of the fine-structure NO absorption bands with an uncertainty of 30 °C – 100 °C, but may be improved after further work or use of the spectral features of other gas components. Uncertainties in the gas temperature measurements can be significant lower, e.g. below 5 °C, by use of the radiance (absolute intensity) from the selected region in a CO₂ emission spectrum. A combined method utilizing simultaneous IR and UV spectra measurements will lead to more accurate and complete results, e.g. gas temperature measurements based on the IR emission and sensitive NO measurements by UV absorption spectroscopy. A combined IR-UV technique is under development in the project “*New IR-UV gas sensor to energy and transport sector*” Energinet.dk, project no. 2007 1 7319.
- A 9-m long probe with UV optical head for fast *in situ* absorption measurements has been developed and successfully tested on the large scale.
- At certain optical depths time-resolved NO absorption features can be distinguished from the complex absorption spectrum (e.g. SO₂ + NO). Water has a minor influence on UV-absorption measurements. The NO detection limit by high-resolution UV-absorption spectroscopy is evaluated and discussed.

6 References

1. L S Rothman et al *J. Quant. Spectrosc. Radiat. Transfer* **96**, 139 (2005) and www.hitran.com
2. Z Lin-Fan, Z Zhi-Ping, Y Xhen-Sheng, Z Wei-Hua, L Xiao-Jing, J Xi-Man, Xu Ke-Zun and L Jia-Ming *Chin. Phys.* **11**, 1149 (2002)
3. B H Armstrong *J. Quant. Spectrosc. Radiat. Transfer* **7**, 61 (1967)
4. M D Di Rosa and R K Hanson *J. Quant. Spectrosc. Radiat. Transfer* **5**, 515 (1994)
5. I I Sobelman, L A Vainshtein and E A Yukov *Excitation and Broadening of Spectral Lines*, Springer, Berlin (1981)
6. H Trad, P Higelin, N Djebaili-Chaumeix, C Mounaim-Rousselle, *J. Quant. Spectrosc. Radiat. Transfer* **90**, 275 (2005)
7. A Fateev and S Clausen “*In situ gas temperature measurements by UV absorption spectroscopy*”, *Int. J. Thermophysics*, electronic Online First article, June 11 (2008) <http://www.springerlink.com/content/c62k5q01228m1584/>
8. S Clausen, K A Nielsen and A Fateev, “Ceramic high temperature gas cell operating up to 1873 K”, 2008 to be submitted to *Meas. Sci. Tech.*
9. J Bak and S Clausen, *J. Quant. Spectrosc. Radiat. Transfer* **61**, 687 (1999)
10. J Mellqvist, A Rosen, *J. Quant. Spectrosc. Radiat. Transfer* **56**, 209 (1996)
11. A Fateev and S Clausen “*In situ fast UV absorption spectroscopy with 9-m long probe on an industrial scale boiler*”, 2008 to be published

